

Ameliorating the Toxic Effect of the Immunosuppressive Drugs (Tacrolimus) on Male Albino Rat Tongue by Mesenchymal Stem Cells Versus Platelet Rich Plasma (Histological, Immunohistochemical and Scanning Electron Microscopic Study)

Amal M. Elshazly^a, Neama M. Taha^b, Asmaa Y. Hussein^c, Naglaa A. Sarg^a

Abstract:

^a Anatomy Department, Faculty of Medicine Benha University, Egypt.

^b Physiology Department, Umm Al-Qura University, Saudi Arabia.

^c Forensic and Toxicology Department, Faculty of Medicine Benha University, Egypt.

Corresponding to:
Dr. Amal M. Elshazly.
Anatomy Department, Faculty of Medicine Benha University, Egypt.
Email:
amal,elshazly79@yahoo.com

Received: 17 November 2022

Accepted: 29 November 2022

Background: Toxic effects on the tongue caused by Tacrolimus remains a major problem. Therefore, the aim of this research was to evaluate the potential therapeutic bone marrow-derived mesenchymal stem cells (MSCs) and platelet rich plasma (PRP) impact on tongue of albino rat. **Materials and Methods:** 40 Albino male rats were divided into four equal groups. Group I (control group) received no treatment. Group II received daily subcutaneous injections of 1 mg/kg/day of Tacrolimus for 30 days. Group III received Tacrolimus for 30 days then a single PRP injection. Group IV received Tacrolimus for 30 days then a single injection of MSCs. In all groups the rats were scarified after sixty days from the beginning of the experiment. For demonstration of the collagen fibers, tongue sections were stained with Mallory Trichrome and were stained with Hematoxylin and Eosin for histological analysis. Electron microscopic scans were used in this study and immunohistochemistry using anti- PCNA primary antibody were used to examine the tongue. **Results:** Histological and immunohistochemical examination of Tacrolimus group tongues showed poorly defined filiform papillae, some epithelial cells appeared degenerated with pyknotic nuclei, however tongue sections of Gr. II and Gr. IV showed marked tongue histological structure improvement and up regulated expression of PCNA, compared to the Gr. II. Scanning electron microscope supported these results. **Conclusion:** MSCs and PRP have good effects in reduction of the toxic effect of Tacrolimus administration on the rat tongue with insignificant difference between the two methods.

Keywords: Tacrolimus; MSCs; PRP; tongue toxicity.

Introduction

Tacrolimus is an immunosuppressive drug (macrolide calcineurin inhibitor) which is effective in reduction of acute and chronic rejection and improvement of renal function over the long-term post-transplant with lower risk factors. Tacrolimus is present in the market as intravenous injection, oral administration and topical ointment.

Tacrolimus has been used in suppressing the inflammation associated with ulcerative colitis which does not respond to high doses of systemic corticosteroids with less side effects ⁽¹⁾. Tacrolimus is used in dermatology in treatment of atopic dermatitis, erosive mucosal lichen planus and Crohn's disease of the mouth ⁽²⁾. Immunosuppressive drugs increase the risk of cancer to a major concern. In organ transplant recipients, malignancy incidence is markedly higher than in general population. Food and Drug Administration (FDA) advised weighing up the risks of treatment against the benefits and they also indicated that these agents should not be used if the patients were immunocompromised ^(3,4).

Tacrolimus has a wide range of drug-drug and food-drug interactions. Because of its variable pharmacokinetics and narrow therapeutic index, monitoring the drug concentration is essential to prevent the risk of over or under immunosuppression ⁽⁵⁾. Side effects include cardiac damage, infection, diabetes mellitus, hypertension, hepatotoxicity and nephrotoxicity ⁽⁶⁾.

Multiple studies have established the efficacy of mesenchymal stromal cells produced from bone marrow (BM-MSCs) in the treatment of the oral mucosa disorders. Stem cells are immature or undifferentiated cells that

may produce daughter cells with comparable characteristics or develop into a variety of cell types. Stem cells are the progenitors of bodily tissue ⁽⁷⁾. Furthermore, platelet-rich plasma (PRP) has been demonstrated to improve the angiogenic response of the wounds of the oral mucosa within the 1st 10 days following surgery ⁽⁸⁾. Consequently, this trial assessed the potential regenerative effect of BM-MSCs and PRP on Tacrolimus induced oral toxicity.

Materials and Methods:

Type of study: Experimental study.

The experimental animals:

This study was done at the Anatomy department in Banha Faculty of Medicine, started in the 26 of August 2022 to 26 of October 2022, and conducted on 40 albino male rats with a mean weight of 200 ± 20 g from the animal house at Banha University's Faculty of Veterinary Medicine. Rats were maintained at an appropriate temperature with a 12-hour light/dark cycle. The animals were kept for ten days and fed on a diet of 10% varied vegetables, 20% dry milk, 20% yellow maize, 50% barley, and tap water prior to the experimental investigation.

Drugs:

The immunosuppressant drug (Tacrolimus) was purchased from (Prograf® – Janssen Cilag, São José dos Campos, SP, Brazil) in the form of 1ml ampules each one contains 5mg Tacrolimus.

Bone marrow derived Mesenchymal Stem cells (BMMSCs):

BMMSCs extract was purchased from the stem cells research unit at Histology Department, Faculty of Medicine, Benha University.

Labeling Of Stem Cells with PKH26

Dye: after isolation of MSCs it was labeled with the PKH26 fluorescent

linker dye during the 4th passage. PKH26 is a red fluorochrome with 567 nm emission and 551 nm excitation. Both proliferative and biological activities are preserved in the labeled cells. Therefore, the linker is suitable for long-term in vivo cell tracking, in vitro cell labeling, and in vitro cell proliferation studies. The dye is stable and will divide proportionally as the cells divide. Detection of the homing of injected cells in the rat's tongue: At the completion of the experiment, a fluorescence microscope was used to identify the PKH26-stained cells in the rat's tongue, revealing that the injected cells had engrafted into the (Gr IV) tongue^(9, 10).

PRP Preparation protocol:

Extraction of blood from each rat of the experiment was done using vacuum tubes containing 10% sodium citrate. A technique including two folds centrifugation was used to create the PRP. Group III rats were injected with their own platelets⁽¹¹⁾.

Experimental protocol: 40 rats were equally classified into 4 groups. Group I (Gr. I): control group had no treatment.

Group II (Gr. II): For thirty days, each rat was injected subcutaneously with 0.2 ml of 1 mg/kg/day Tacrolimus once daily. Rats were weighed weekly⁽¹²⁾. This dose leads to peak plasma concentrations of Tacrolimus of approximately 11.2 ng/ml⁽¹³⁻¹⁵⁾.

Group III (Gr. III): As in group II, rats received Tacrolimus for 30 days, followed by a single dosage of PRP injected into the right lateral border of the tongue after sedating rats by ether inhalation. The injection was administered using a 1 mL insulin syringe with a 27-gauge, 1/2 needle (BD Nokor).

Group IV (Gr. IV): Rats received Tacrolimus for 30 days as in group two

then a single dose of BMMSCs 1×10^6 cells administrated by intravenous injection at tail vein.

Sample Preparation:

After 60 days from the beginning of the experiment, all the rats received an anesthetic overdose (0.86 mg/kg sodium pentobarbital intraperitoneally) and slaughtered by cervical dislocation. The mouths of the rats were opened wide, and the tongues were excised using sharp pair of scissors. Tongues were fixed, processed, embedded in paraffin, sectioned, and stained with Hematoxylin and Eosin (H&E) for histological examination. Mallory Trichrome stain for demonstration of collagen fibers and immunohistochemically using anti-PCNA primary antibody. The tongues were examined also by scanning electron microscope.

Histological study: Tongues were removed, preserved in 10% formalin, and then transformed into paraffin blocks. By using a rotary microtome (LEICA RM 2125, UK). These blocks were sectioned to a thickness of 5 m, then stained with H&E, a standard histological stain, and Mallory Trichrom (MT), a specialized stain used to analyze collagen fibers, were then applied to the blocks⁽¹⁶⁾. Histo-morphometric data was obtained by a light microscope (Olympus-Bx; 4500) coupled to a digital camera (Nikon-Coolpix; 4500) with objective lens magnifications of 200 and 400 to inspect the slides.

Immunohistochemistry: Sections (5µm thickness) were dewaxed, rehydrated, and washed with PBS. The sections were incubated overnight at 4°C in a humid chamber with the primary anti-proliferating cell nuclear antigen (PCNA) antibody (Mouse monoclonal antibody, 1:200 dilution, Ab-1 (Clone PC10), CAT. # MS-106-

R7, Lab Vision Corporation, USA) in PBS. Thereafter, it was washed in PBS buffer, and co-incubated with biotinylated secondary antibody (Dako North America, Inc., CA, USA) for 1hr. at room temperature. 10 min of Streptavidin peroxidase addition was followed by 3 PBS washes. Using 3, 3'diaminobenzidine (DAB)-hydrogen peroxide as a chromogen, the immunoreactivity was observed. The sections were finally counterstained with Mayer's Hematoxylin. Negative control sections were treated without addition of primary antibodies⁽¹⁷⁾.

Under a light microscope, all slides were examined for histological examination and identification of the specific brown reaction product of the DAB substrate in the immune-stained sections.

Morphometric study:

Image analysis software (Image j. version 1.46) was used to calculate the proportion of collagen fiber deposition and PCNA immune-positive staining in 10 randomly selected 200x magnification microscopic fields for each specimen.

Ethical approval:

This experimental study was reviewed and approved in accordance with the Research Ethical Committee Recommendations of Faculty of Medicine, Benha University, (Rc.42.10.2022).

Statistical analysis: SPSS version 20 was used. Using One-way analysis and a t-test, the mean and standard deviation (S.D) of the data were calculated. Significance levels were deemed at $p \leq 0.05$.

Scanning electron microscopy:

Samples were fixed in 2.5% glutaraldehyde in 0.1 M phosphate buffered glutaraldehyde pH 7.4 at 4C for 2h. The fixed samples were washed 3 times with PBS (10 min. each). After

being post-fixed in 1 % Osmic acid for 30 minutes, the samples were dehydrated by an escalating series of ethyl alcohol (30, 50, 70, and 90 percent) infiltrated with acetone for 30 minutes⁽¹⁸⁾. Before being gold-coated in an SPI- Module (Sputter Carbon / Gold Coater), the samples were dried in a Critical Point Dryer (Tousimis Autosamdri – 815 Coate) and mounted on aluminium stubs. At Banha University's electron microscopy unit, the samples were evaluated using a scanning electron microscope (JSM-6510 LV) (JEOL, Japan).

Results:

Histological results: Hematoxylin and Eosin staining:

Tongue sections from the control group (Group I) were stained with Hematoxylin and Eosin, revealing a normal architecture with a regular distribution and orientation of filiform papillae with characteristic tapering ends, a normal amount of keratinized stratified squamous epithelial covering, and a thin underlying lamina propria. The tongue muscle fibers were running in different directions underneath the papillae. Fungiform papillae were coated by keratinized stratified squamous epithelium, and their dorsal surfaces contained well-defined barrel-shaped taste buds (Fig., 1).

Group II (Tacrolimus group) tongue sections had poorly defined filiform papillae with epithelial hyperkeratosis and a decrease in filiform papillae height with blunt edges. The epithelial cells of filiform papillae showed cellular pleomorphism and nuclear hyperchromatism. Some epithelial cells appeared to degenerate with pyknotic nuclei which were surrounded by vacuolated cytoplasm. The lamina propria was infiltrated by inflammatory

cells. There were ill defined papillae with epithelial hyperplasia with deeply stained nuclei and cytoplasmic vacuoles. Some epithelial cells appeared to degenerate with pyknotic nuclei. The taste buds showed irregular arrangement with separated cells (Fig., 2).

However, sections from PRP group (Gr. III) showed almost normal histological of filiform papillae with regular arrangement and shape and normal papillary connective tissue. Epithelial hyperplasia and hyperkeratosis were observed with few disfigured papillae with blunt appearance ends in-between and a nearly normal pattern of epithelial ridges. The fungiform papillae appeared nearly normal with few degenerated epithelial cells. The cells of taste buds

showed almost regular arrangement (Fig., 3).

The tongue sections from MSC rats' tongues (Gr. IV) showed almost normal histological appearance of filiform papillae and fairly normal papillary connective tissue. Epithelial hyperplasia and hyperkeratosis were observed with thin keratin layer over the stratified squamous epithelial cover. The fungiform papillae appeared nearly normal with few degenerated epithelial cells having pyknotic nuclei. The cells of taste buds showed almost regular arrangement (Fig., 4).

One week after transplantation of MSCs into the tongue of a rat, cells tagged with PKH 26 exhibit significant red autofluorescence (Gr. IV) (Fig.,5).

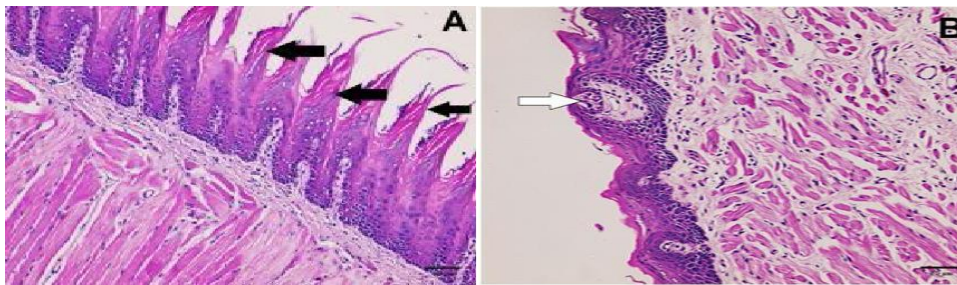


Fig. (1): Photomicrograph of rat tongue dorsal surface of (Gr. I) the control group showing (A): normal architecture with regular distribution and orientation of filiform papillae with characteristic tapering ends (black arrows), normal amount of keratinized stratified squamous epithelial covering and thin underlying lamina propria. The tongue muscle fibers are running in different directions underneath the papillae (B): Fungiform papilla is covered by keratinized stratified squamous epithelium and a well-defined barrel-shaped taste bud is present on its dorsal surface (white arrow). (H&E A and B x200).

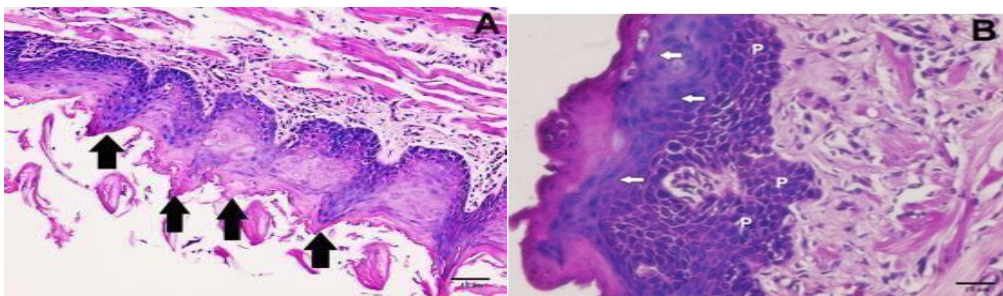


Fig. (2): Photomicrograph of the dorsal surface of the tongue of (Gr. II) Tacrolimus group showing (A): ill-defined filiform papillae with epithelial hyperkeratosis and an apparent decrease in the height of the filiform papillae with blunt ends (black arrows). (B): The epithelial cells of filiform papillae show cellular pleomorphism and nuclear hyperchromatism. Some epithelial cells appear degenerated with pyknotic nuclei (white arrows). The lamina propria is infiltrated with inflammatory cells. An ill-defined fungiform papilla with epithelial hyperplasia, with deeply stained nuclei the taste bud shows irregularly arranged and separated cells (arrowhead). (H&E Ax200 and B x400).

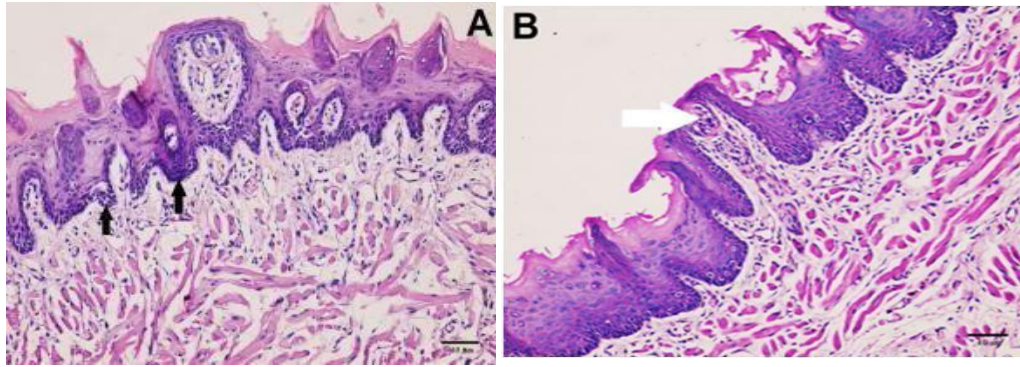


Fig. (3): Photomicrograph of the dorsal surface of rat tongue of PRP group (Gr.III) showing (A): almost normal histological appearance of filiform papillae with regular arrangement and shape and fairly normal papillary connective tissue. Epithelial hyperplasia and hyperkeratosis are observed (black arrows). with a few disfigured papillae and nearly normal pattern of epithelial ridges. (B): The fungiform papilla appears nearly normal with few degenerated epithelial cells. The cells of the taste bud show almost regular arrangement in its upper surface (white arrow) (H&E A and B x200).

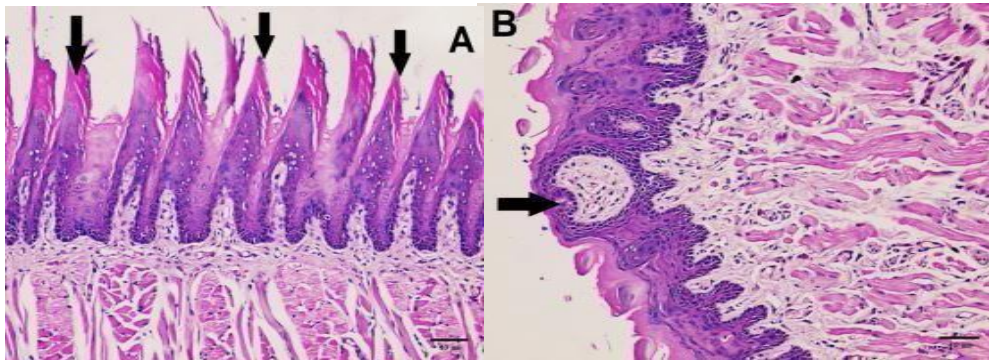


Fig. (4): Photomicrograph of the dorsal surface of MSC rats' tongues (Gr. IV) showing (A): almost normal histological appearance of filiform papillae and fairly normal papillary connective tissue (black arrows). Epithelial hyperplasia and hyperkeratosis are observed. thin keratin layer over the stratified squamous epithelial cover (B): The fungiform papilla appears nearly normal with few degenerated epithelial cells. The cells of the taste bud show almost regular arrangement (black arrow) (H&E A and B x200).

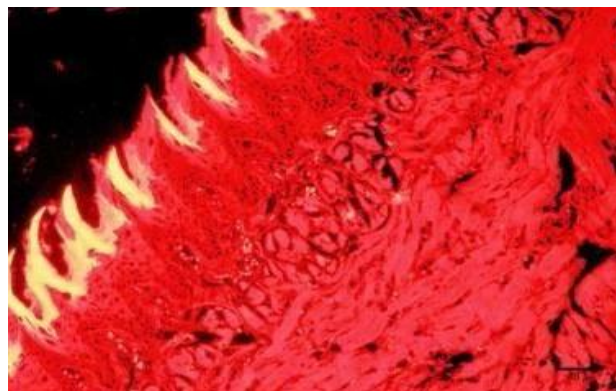


Fig. (5): Cells labeled with PKH 26 showing strong red auto fluorescence at 1 week following transplantation of (MSCs) in the rat's tongue.

Mallory's Trichrome stain:

Deposition of collagen fiber increased between the muscle fibers and in the lamina propria (Fig., 6A) in the Tacrolimus group (Gr. II) compared to the control group (Gr. I) (Fig., 6B). Deposition of collagen fiber decreased between the muscle fibers and in the lamina propria in the PRP group (Gr. III) (Fig., 6C). In addition, the MSCs group (Gr. IV) demonstrated a reduction in the deposition of collagen fiber between the muscle fibers and in the lamina propria (Fig., 6D).

Results of Immuno-histochemical staining:

PCNA: Histological slices of the tongues of the controls demonstrated moderate to strong PCNA staining reactivity mostly in the basal and parabasal cells of the surface epithelium, suggesting normal proliferation of the cells of the dorsal surface of the tongue. All the basal cells were positively stained (Fig., 7A). The sections of the tongues of Gr. II

(tacrolimus group) showed low expression of PCNA in the basal layer of the epithelium of the dorsal surface ranging from negative to weakly positive staining reaction which indicated a decrease in proliferation of basal and parabasal cell layers denoting marked decrease in cell renewal and turnover rate. Most of the basal cells were negatively stained (Fig., 7B). The sections of the rats' tongues that were treated with platelet rich plasma Gr. III (PRP group) showed moderately to strongly positive PCNA expression in the basal and parabasal cells of the dorsal surface of the tongue. However not all the basal cells were positively stained (Fig.,7C). The basal and parabasal cells of the dorsal surface of the tongues of rats who received an injection of stem cells, group IV MCS group, exhibited moderate to significant PCNA expression (Fig., 7D).

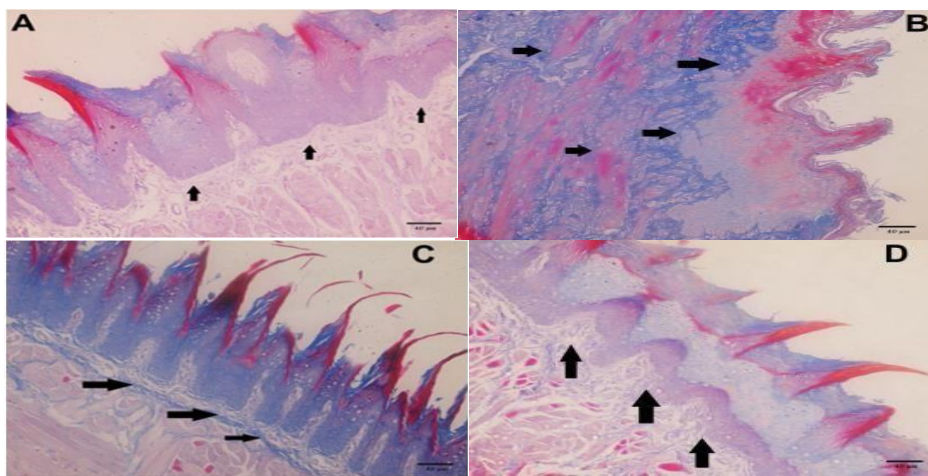


(Fig. 6): A photomicrograph of dorsal surface of the rat tongue (A): from control group (Gr. I) showing few collagen fiber deposition in between the muscle fiber and in the lamina propria. Notice the collagen fiber appear blue (black arrows). (B): Rat tongue dorsal surface of anterior two thirds from tacrolimus group (Gr II) exhibiting increase in deposition of collagen fiber (black arrows) in the lamina propria and in between the muscle fibers. (C) The dorsal surface of a tongue from the PRP group (Gr. III) demonstrates a reduction in collagen fiber deposition in between the muscle fibers and in the lamina propria (black arrows). (D) Rat tongue dorsal surface from (MSCs) group (Gr. IV) demonstrates decrease in collagen fibers deposition (black arrows) in between the muscle fibers and in the lamina propria and. (A, B, C and D Mallory's trichrome stain $\times 200$).

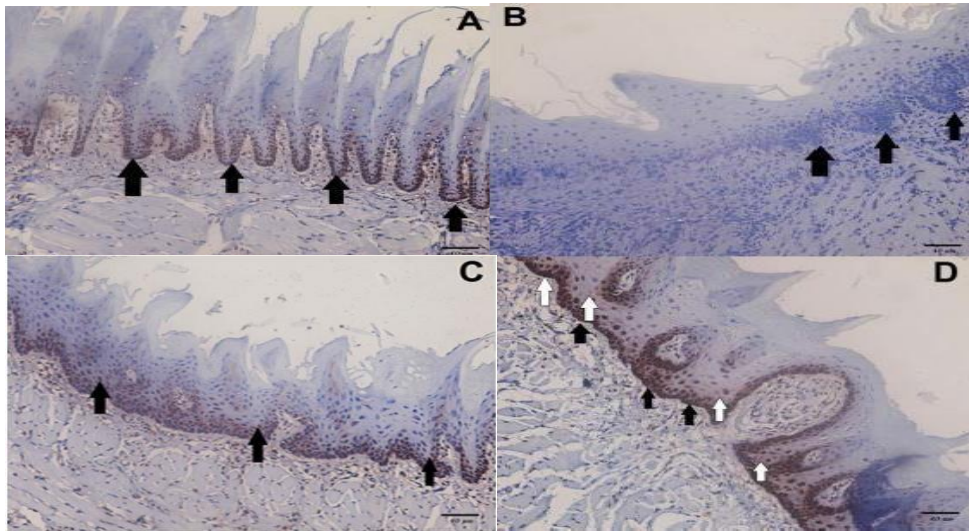


(Fig. 7): Photomicrograph of the dorsal surface of the anterior 2/3 of the rat's tongue (A): from group one (Gr. I) control group showing a positive brown nuclear immunoreaction for PCNA in many epithelial cells in the basal and parabasal layers of the tongue mucosa (black arrows) with few -ve nuclei and mild reaction in the lamina propria.(B) The dorsal surface of the anterior 2/3 of the rat's tongue from group two (Gr. II) (tacrolimus group) showing a negative nuclear immunoreaction for PCNA in epithelial cells in the basal and parabasal layers of the tongue mucosa (black arrows).(C) The dorsal surface of the anterior 2/3 of the rat's tongue from group three (Gr. III) PRP group showing a positive nuclear immunoreaction for PCNA in many epithelial cells in the basal and parabasal layers of the tongue mucosa with few -ve nuclei (black arrows) and mild reaction in the lamina propria.(D) The dorsal surface of the anterior 2/3 of the rat's tongue from group four (Gr. IV) MCS group showing PCNA immunolocalization in the tongue strongly positive nuclei in the basal cells and parabasal layers of the tongue mucosa (black arrows) with few -ve nuclei (whit arrows) and mild reaction in the lamina propria. [A, B, C and D PCNA immunostaining, X200].

Morphometric results:

Table (1) and histogram (1) illustrate the mean area percent of deposition of collagen fiber in tongue sections for all groups. In group II, the mean area percentage of deposition of collagen fiber was markedly higher compared to group I. In comparison to group II, the mean area percentage of deposition of collagen fiber significantly decreased in groups III and IV. The mean area percentage of collagen fibers deposition in group IV was

insignificantly lower than in group III (Table 2 and histogram 2). The mean area percentage of PCNA expression was significantly lower in group II than in group I. The mean area percentage of PCNA expression was significantly higher in groups III and IV compared to group II. Group IV had a higher mean area percentage of deposition of collagen fiber than group III, although the difference was not statistically significant.

Table (1): Mean values of area percent of Mallory’s trichrom stain in the 4 groups.

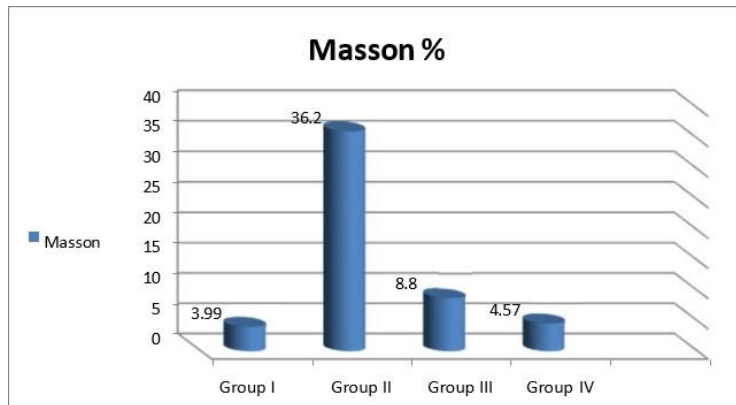
Mean % ± S.D	Group I	Group II	Group III	Group IV
Masson%	3.99 %± 2.1	36.2% ± 3	8.8% ± 1.2	4.57% ± 0.76
Significance	With group II	With groups I, III & IV	With group II	With group II
P value ≤0.05				
P- value	I versus II = 0.000 I versus III = 0.064 I versus IV = 0.567	II versus I = 0.000 II versus III = 0.000 II versus IV = 0.000	III versus I = 0.064 III versus II = 0.000 III versus IV = 0.360	IV versus I = 0.567 IV versus II = 0.000 IV versus III = 0.360

Using one way ANOVA with Tukey’s tests to identify statistically significant pairs ; statistically significant: $p < 0.05$.

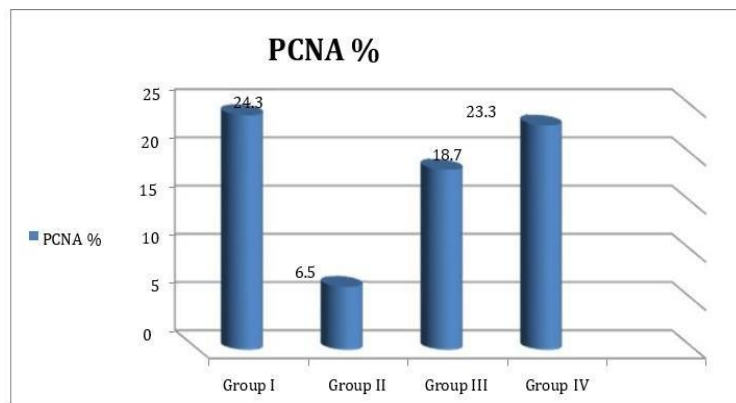
Table (2): Mean values of area percent PCNA immunoreactivity in the 4 groups using.

Mean % ±S.D	Group I	Group II	Group III	Group IV
PCNA %	24.3 %± 3.3	6.5 %± 0.96	18.7 %± 1	23.3% ± 2.7
Significance	With group II	With groups I, III& IV	With group II	With group II
P value ≤ 0.05				
P- value	I versus II=0.000 I versus III=0.314 I versus IV=0.758	II versus I= 0.000 II versus III= 0.01 II versus IV= 0.000	III versus I = 0.314 III versus II = 0.001 III versus IV= 0.734	IV versus I = 0.758 IV versus II = 0.000 IV versus III = 0.734

Using one way ANOVA with Tukey’s tests to identify statistically significant pairs ; statistically significant: $p < 0.05$.



Histogram (1): Mean values of area percent of collagen fibers deposition in the four groups.



Histogram (2): Showing mean values of area percent of PCNA immunoreactivity in the four groups.

Results of Scanning electron microscope:

The control rat tongues showed regular parallel rows of long conical filiform papillae with tapering ends. The papillae showed uniform arrangement with antero-posterior inclination. Broad dome shaped fungiform papillae having flattened smooth upper surfaces were found in between the filiform papillae. Mushroom-like fungiform papillae were interposed in between the numerous filiform ones with well-defined taste orifices seen on their top surfaces (Fig., 8).

In Tacrolimus group rats' tongues, the filiform papillae showed disorganized orientation, inclination and markedly desquamated filiform papillae. The area of fusion of the papillae was short, thin and desquamated. There were many damaged filiform papillae some of them showed keratinized blunt ends. Fungiform papillae with rough upper surfaces and ill-defined taste pores were noted. These papillae appeared distorted with wrinkled keratinized epithelial covering with depressed top surface. The interpapillary areas were rough and prominent (Fig.,9).

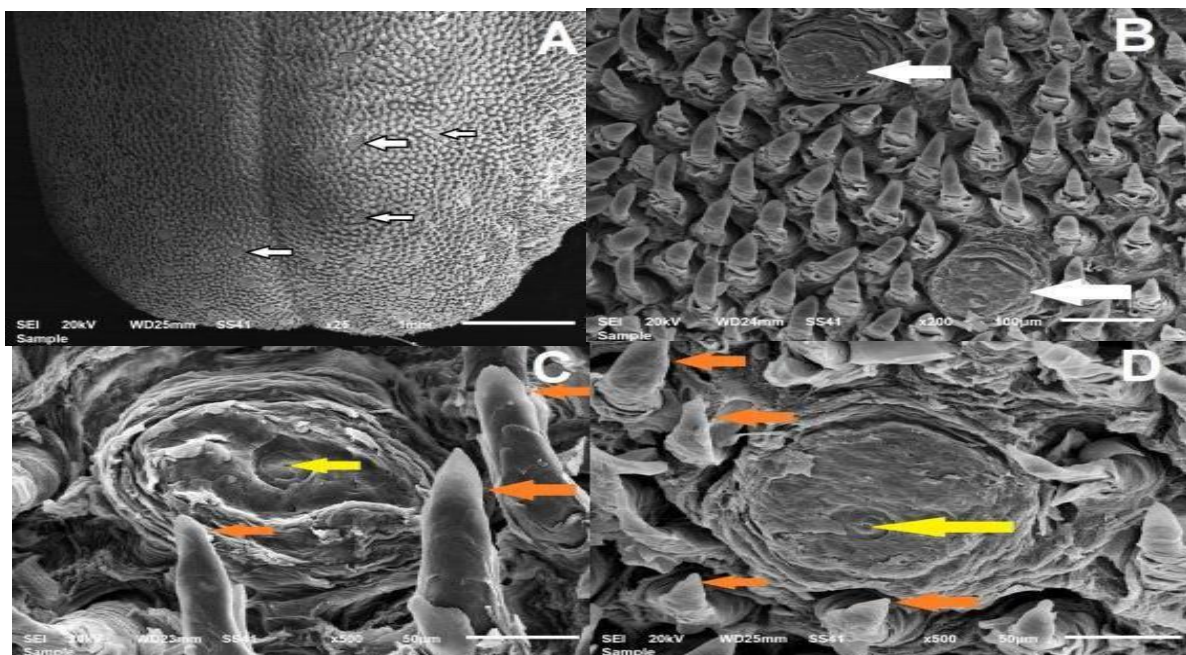


(Fig. 8): Scanning electron micrographs of the control rat tongue showing (A&B): regular parallel rows of long conical filiform papillae with tapering ends. The papillae show uniform arrangement with antero-posterior inclination. Notice a broad dome shaped fungiform papilla having a flattened smooth upper surface. (C& D) conical shaped filiform papillae with their tapering tips that pointed into the same direction (red arrows). Mushroom-like fungiform papillae are interposed in between the numerous filiform ones. A well-defined taste orifice can be seen on its top surface (yellow arrow) (SEM A X25, B X200, C&D X 500)

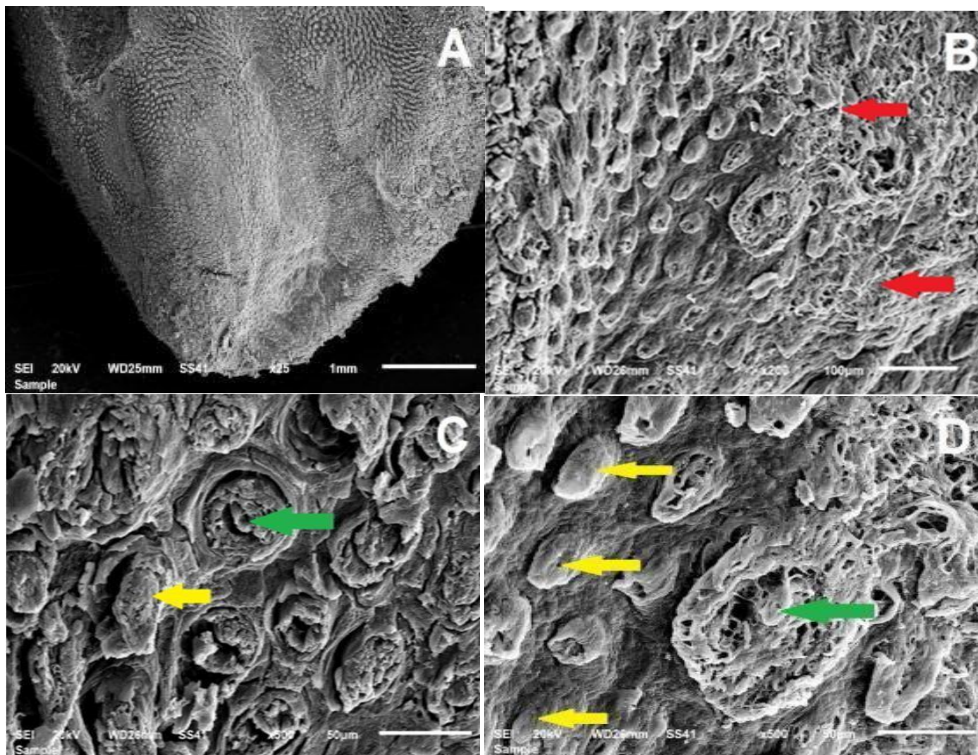


(Fig.9): Scanning electron micrographs of Tacrolimus rats' tongues. (A&C) The filiform papillae show disorganized orientation and inclination and showing markedly desquamated filiform papillae. Note the area of fusion of the papillae (red arrows) (C&D) short thin, desquamated and damaged filiform papillae Some filiform papillae show keratinized blunt ends (yellow arrows), fungiform papilla with a rough upper surface and an ill-defined taste pore (green arrow), The interpapillary areas were rough and prominent. Notice the irregular shape of filiform papillae. The fungiform papilla appears distorted with wrinkled keratinized epithelial covering with depressed top surface. (SEM A X25, B X200, C&D X 500).

The rats' tongues of the PRP group showed partial restoration of normal appearance of filiform papillae with scattered fungiform papillae. The filiform papillae appeared nearly normal and more regular with tapering ends and normal interpapillary distance. There were almost normal fungiform papillae with depressed surfaces and regular smooth epithelial covering with normal appearance of taste buds. Some filiform papillae appeared blunt (Fig.,10)

The rats' tongues of the MSC group showed restoration of the near normal

appearance of filiform papillae with scattered fungiform papilla. The filiform papillae appeared nearly normal and more regular with tapering ends and normal interpapillary distance. Also, there were regular arrangement and shape of the filiform papillae with regular distribution of normal fungiform papillae in-between. The fungiform papillae appeared with depressed surfaces and regular smooth epithelial covering and normal taste pits (Fig.,11).

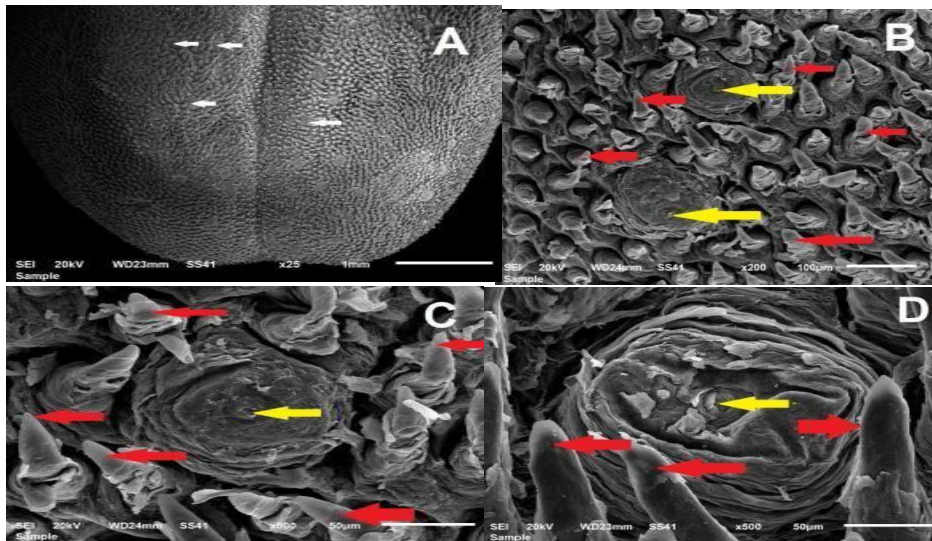


(Fig. 10): Scanning electron micrographs of the PRP rats' tongues showing (A): partial restoration of normal appearance of filiform papillae with scattered fungiform papillae (white arrow). (B, C and D) The filiform papillae appear nearly normal and more regular with tapering ends (red arrows) and normal interpapillary distance. almost normal fungiform papilla with depressed surface and regular smooth epithelial covering with normal appearance of taste bud (yellow arrow). Some filiform papillae still appear blunt (SEM A X25, B X200, C&D X 500)

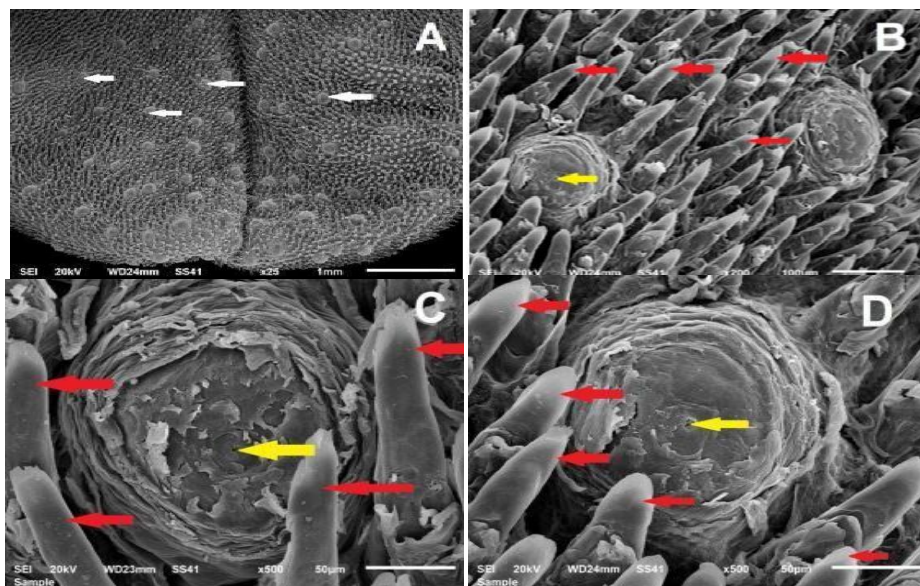


(Fig. 11): Scanning electron micrographs of the MSC rats' tongues showing (A): nearly normal restoration of normal appearance of filiform papillae with scattered fungiform papillae (white arrows). The filiform papillae appear nearly normal and more regular with tapering ends and normal interpapillary distance. (B, C and D) regular arrangement and shape of the filiform papillae with regular distribution of normal fungiform papillae (red arrows) in-between. Notice a few short and thin filiform papillae almost normal fungiform papilla with depressed surface and regular smooth epithelial covering and normal taste pit (yellow arrow) (SEM A X25, B X200, C&D X 500).

Discussion:

The results of the current histological research revealed that Tacrolimus produces variable degrees of atrophic changes in the epithelium and papillae of the tongue. There was loss of the normal shape of each tongue papilla and degeneration of the cells of taste buds inside it. The epithelium of the basal and spinous cell layers showed cytoplasmic vacuolization. Also, the epithelial cells of the serous and mucous acini showed marked vacuolization. Collagen fibers in the subepithelial lamina propria of the tongues which suffered dissociation were seen in the group treated with tacrolimus. Mallory's Trichrome stained sections confirmed the marked degeneration and dissociation of the collagen fibers in the tissues under investigation. This result is consistent with prior research indicating that oral mucositis (OM) is a common and often severe complication of posttransplant conditioning treatment that results in painful oral and gastrointestinal mucosal ulcerations⁽¹⁹⁾. Karin et al.⁽²⁰⁾ remarked that attempts to treat graft-versus-host disease (GVHD), such as the use of novel combinations of immunosuppressive drugs, may have unintended side effects. The development of oral lesions is hazardous. Additionally, OM injuries may take longer to recover. Damage to cells is the result of a complicated cascade that begins with cell death and the development of reactive oxygen species, continues through numerous phases in which biological processes is accelerated, and concludes with the formation of mucosal ulcers⁽²¹⁾. Denise⁽²²⁾ found that treatment with Tacrolimus is associated with increased oral fibrous growth.

In the current study, treatment by PRP restored the normal tongue papillae architecture after treatment with Tacrolimus. The detected improvement in histological and scanning electron microscope (SEM) features agreed with

Elsaadany et al.⁽²³⁾ who concluded the effects of PRP treatment in prevention of the atrophy in tongue dorsal surface epithelium after Tacrolimus treatment. The presence of growth factors in PRP that promote cell proliferation, chemotaxis, differentiation, extracellular matrix production, and angiogenesis, all of which contribute to the healing of radiation-induced mucositis, may explain this therapeutic effect^(24,25). Marek et al.⁽²⁶⁾ determined that PRP exhibited a unique angiogenesis and linked it to coagulation factors and platelet activity. Platelets can store and release numerous angiogenic substances, as platelet-derived epidermal growth factor (PD-EGF), basic fibroblast growth factor (bFGF), platelet-derived growth factor (PDGF), transforming growth factor beta, VEGF and angiopoietins. In addition, PRP performed a significant impact in the recruitment, proliferation, and differentiation of tissue-regenerating cells^(27,28). Maria et al.⁽²⁹⁾ clinical findings indicated that the duration of radiation-induced OM was reduced by 72% after using the therapy of syngeneic freshly cultured adipose MSCs which decreased via increasing the clinically significant ulceration latency and accelerating its healing; our histology data support these conclusions.

Schmidt et al.⁽³⁰⁾ discovered that bone marrow IV transplantation and bone marrow derived MSCs significantly decreased the radiation-induced OM ED50 in a single- dose model. Due to the low quantity of PKH26-labeled BM-MSCs transplanted into the mucosa of the tongue in our investigation, regeneration of lost epithelial cells by trans-differentiation seems unlikely to be the primary therapeutic method. Nonetheless, the advantages of MSC seen in these trials might be the result of paracrine factor release and synergistic effects. Stem cells are used to treat mouth ulcers and wound healing by combining cell migration and proliferation with

extracellular matrix deposition, remodeling, and angiogenesis. BM-MSCs are self-renewing, expandable stem cells that stimulate tissue regeneration and wound repair by inhibiting pro-inflammatory cytokines and stimulating the production of soluble antiapoptotic, proangiogenic, and antioxidant components⁽³¹⁾.

According to Dong et al., MSCs generate and release several cytokines and growth factors, including HGF, IL-11, IGF-I, and FGF-2⁽³²⁾. Each of these factors promotes cell proliferation, inhibits epithelial cell apoptosis, or both⁽³³⁾, promoting mucosal healing. Due to the flexibility of stem cells, stem/progenitor cell transplantation has been found in a number of investigations⁽³⁴⁾ to promote cancer angiogenesis, proliferation, and metastasis, whilst in other studies stem/progenitor cells suppressed tumor activity⁽³⁵⁾.

Conclusion:

There is no significant difference between PRP and Tacrolimus MSCs in terms of their ability to reduce the toxic effects of Tacrolimus administration on the tongue.

Conflicts of Interest: The authors declare no conflict of interest.

References:

1. IriaSeoane-Viaño, JunJieOng, AsteriaLuzardo-Álvarez, MiguelGonzález-Barcia, AbdulW.Basit, FranciscoJ.Otero-Espinar, et al. 3D printed tacrolimus suppositories for the treatment of ulcerative colitis. *Asian J Pharm Sci*, 2021; 16 (1):110-119.
2. David Aung-Din, BS Michael Heath, Todd Wechter, Abigail Cline, Steven R. Feldman, Joseph L. Jorizzo,. Effectiveness of the Tacrolimus Swish-and-Spit Treatment Regimen in Patients With Geographic Tongue. *JAMA Dermatology*, 2018; 154(12):1479-1482.
3. Alejandro Arana, Anton Pottegård, Josephina G Kuiper, Helen Booth, Johan Reutfors, Brian Calingaert, et al. Long-Term Risk of Skin Cancer and Lymphoma in Users of Topical Tacrolimus and Pimecrolimus: Final Results from the Extension of the Cohort Study Protopic Joint European Longitudinal Lymphoma and Skin Cancer Evaluation (JOELLE). *Clinical Epidemiology*,2021; 13:1141-1151
4. Wiseman AC. Immunosuppressive medications. *Clin J Am Soc Nephrol*, 2016; 11:332–343.
5. Mercè Brunet, Teun van Gelder , Anders Åsberg , Vincent Haufroid , Dennis A Hesselink , Loralie Langman et al. Therapeutic Drug Monitoring of Tacrolimus-Personalized Therapy: Second Consensus Report.*Drug Monit*, 2019; 41(3):261-307
6. Brian J Nankivell , Chow H P'Ng, Philip J O'Connell, Jeremy R Chapman. Calcineurin Inhibitor Nephrotoxicity Through the Lens of Longitudinal Histology: Comparison of Cyclosporine and Tacrolimus Eras Transplantation Aug,2018; 100(8):1723-31.
7. Omoko Kobayashi, Daisuke Torii, Takanori Iwata, Yuichi Izumi, Masanori Nasu & Takeo W. Tsutsui. Characterization of proliferation, differentiation potential, and gene expression among clonal cultures of human dental pulp cells. *Human Cell*, 2020; volume 33, pages490–501
8. Mary Moheb Ramzy ,Tarik Ahmed Essawy, Ali Shamaa and Saher Sayed Ali Mohamed. Evaluation of the Effect of Platelet Rich Plasma on Wound Healing in the Tongue of Normal and Streptozotocin-induced Diabetic Albino Rats: Histological, Immunohistochemical, and Ultrastructural Study.*j Med Sci*, 2020; 25:8(A).666-689.
9. S. Bruno, C. Grange, F. Collino, M.C. Deregibus, V. Cantaluppi, L. Biancone, et al. Microvesicles derived from mesenchymal stem cells enhance survival in a lethal model of acute kidney injury, *PLoS One*,2012; 7 (3).
10. Alexandra Kelp, Tanja Abruzzese, Svenja Wöhrle, Viktoria Frajs and Wilhelm K Aicher. Labeling Mesenchymal Stromal Cells with PKH26 or VybrantDil Significantly Diminishes their Migration, but does not affect their Viability, Attachment, Proliferation and Differentiation Capacities. *Journal of Tissue Science & Engineering*,2017; 8:2.
11. Yan Huang, Michael M Bornstein, Ivo Lambrichts, Hai-Yang Yu. Platelet-rich plasma for regeneration of neural feedback pathways around dental implants: a concise review and outlook on future possibilities..*International journal of oral science*,2017; (9) 1–9,
12. Karl WMollisonThomas AFeyRuth AKrauseJanet MAndrewsPat TBretheimPatrick KCusickGin CHsiehJay RLuly. Nephrotoxicity studies of the immunosuppressants tacrolimus (FK506) and ascomycin in rat models.*Toxicology*, 1998; 125: (2–3)169-181.
13. Li S, Louis LB 4th, Kawaharada N, Yousem AS, Pham SM. Intrathymic inoculation of donor bone marrow induces long-term acceptance of

- lung allografts. *Ann Thorac Surg*, 2003; 75:257-263.
14. Muramatsu K, Kurokawa Y, Youn-Xin S, Bishop AT, Doi K. Cell traffic between donor and recipient following rat limb allograft. *J Orthop Res*, 2005; 23:181-187.
 15. Voggenreiter G, Siozos P, Hunkemöller E, Heute S, Schwarz M, Obertacke U. Immunosuppression with FK506 has no influence on fracture healing in the rat. *Bone*, 2005; 37:227-233.
 16. S.Kim Suvarna, Chistopher. Layton and John D. Bancroft. *Bancroft,sTheory and Practice of Histological Techniques*, 2019; 126–138.
 17. Ramos-Vara JA, Kiupel M, Baszler T, Bliven L, Brodersen B, Chelack B. et al. Suggested guidelines for immunohistochemical techniques in veterinary diagnostic laboratories. *J Vet Diagn Invest*, 2008; 20: 393–413.
 18. Golding C, Lamboo L, and Beniac D. The scanning electron microscope in microbiology and diagnosis of infectious disease. *Sci Rep*, 2016; 6:26516.
 19. Garming Legert, K. , Remberger, M. , Ringdén, O. , Heimdahl, A. , & Dahllöf, G. Reduced intensity conditioning and oral care measures prevent oral mucositis and reduces days of hospitalization in allogeneic stem cell transplantation recipients. *Supportive Care in Cancer*, 2014; 22(8): 2133–2140.
 20. Karin Garming Legert, Olle Ringdén, Mats Remberger, Johan Törlén, Jonas Mattsson, and Göran Dahllöf . Oral mucositis after tacrolimus/sirolimus or cyclosporine/methotrexate as graft-versus-host disease prophylaxis. *Oral Dis.*, 2021; 27(5): 1217–1225.
 21. Villa, A. , Aboalela, A. , Luskin, K. A. , Cutler, C. S. , Sonis, S. T. , Woo, S. B. , et al. Mammalian target of rapamycin inhibitor-associated stomatitis in hematopoietic stem cell transplantation patients receiving sirolimus prophylaxis for graft-versus-host disease. *Biology of Blood and Marrow Transplantation*, 2018; 21(3), 503–508.
 22. Denise Kissell. Effects of Immunosuppressiv Medications on Oral Health. *Dimensions of Dental Hygiene*, 2021; 19(11)32-35.
 23. Elsaadany B, El Kholy S, El Roubay D, Rashed L, Shouman T. Effect of Transplantation of Bone Marrow Derived Mesenchymal Stem Cells and Platelets Rich Plasma on Experimental Model of Radiation Induced Oral Mucosal Injury in Albino Rats. *Int J Dent*, 2017; 86(34): 540.
 24. Riley P, Glenny AM, Worthington HV, Littlewood A, Fernandez Mauleffinch LM, Clarkson JE, et al. Interventions for preventing oral mucositis in patients with cancer receiving treatment: cytokines and growth factors. *Cochrane Database of Systematic Reviews*, 2017; 11: 25.
 25. Chater C. · Bauters A. · Beugnet C. · M'Ba L. · Rogosnitzky M. · Zerbib P. intraplatelet Vascular Endothelial Growth Factor and Platelet-Derived Growth Factor: New Biomarkers in Carcinoembryonic Antigen-Negative Colorectal Cancer?. *Gastrointest Tumors*, 2018; 5:32–37.
 26. Marek Z. Wojtukiewicz, Ewa Sierko, Dominika HempelStephanie C. Tucker & Kenneth V. Honn. Platelets and cancer angiogenesis nexus. *Cancer and Metastasis Reviews*, 2017; 36: 249–262.
 27. Tony G. ,WalshPat ,Metharom &Michael C. Berndt. The functional role of platelets in the regulation of angiogenesis. *Platelets*, 2016; 26: 199-211.
 28. Y.ZhuM. YuanH. Y.MengA. Y.WangQ.Y.GuoY. WangJ. Basic science and clinical application of platelet-rich plasma for cartilage defects and osteoarthritis. *Osteoarthritis and Cartilage*, 2013; 21(11): 1627-1637.
 29. O. M. Maria, M. Shalaby, A. Syme, N. Eliopoulos, and T. Muanza. Adipose mesenchymal stromal cells minimize and repair radiation-induced oral mucositis. *Cytotherapy*, 2016; 18(9): 1129–1145.
 30. M. Schmidt, A. Piro-Hussong, A. Siegemund, P. Gabriel, and W. Dorr. Modification of radiation-induced oral mucositis (mouse) by adult stem cell therapy: single-dose irradiation. *Radiation and Environmental Biophysics*, 2014; 53(4): 629 – 634.
 31. R. Zhang, Y. Liu, K. Yan. Anti-inflammatory and immunomodulatory mechanisms of mesenchymal stem cell transplantation in experimental traumatic brain injury. *Journal of Neuroinflammation*, 2013; 10: 106.
 32. Nádia de Cássia Noronha, Amanda Mizukami, Carolina Caliári-Oliveira, Juçara Gastaldi Cominal, José Lucas M. Rocha, Dimas Tadeu Covas, et al. Priming approaches to improve the efficacy of mesenchymal stromal cell-based therapies. *Stem Cell Research & Therapy*, 2019; 10: 131
 33. De Boeck, K. Narine, W. De Neve, M. Mareel, M. Bracke, and O. De Wever. Resident and bone marrow-derived mesenchymal stem cells in head and neck squamous cell carcinoma. *Oral Oncology*, 2010; 46(5):336–342.
 34. H. Klopp, A. Gupta, E. Spaeth, M. Andreeff, and F. Marini. Concise review: dissecting a discrepancy in the literature: do mesenchymal stem cells support or suppress tumor growth. *Stem Cells*, 2011; 29(1): 11–19.

To cite this article: Amal M. Elshazly, Neama M. Taha, Asmaa Y. Hussein, Naglaa A. Sarg. Ameliorating the Toxic Effect of the Immunosuppressive Drugs (Tacrolimus) on Male Albino Rat Tongue by Mesenchymal Stem Cells Versus Platelet Rich Plasma (Histological, Immunohistochemical and Scanning Electron Microscopic Study. BMFJ XXX, DOI: 10.21608/bmfj.2024.175374.1711.